γ Radiation Image Denoising Based on Speckle Splitting

Hao Deng
Southwest University of Science and Technology
Hua Zhang (swustai@163.com)
Southwest University of Science and Technology
Hao Zhao
University of Science and Technology of China
Hai Wang
Southwest University of Science and Technology

Research Article

Keywords: γ radiation, speckle noise, image denoising, speckle splitting, NLM

Posted Date: May 26th, 2022

DOI: https://doi.org/10.21203/rs.3.rs-1656465/v1

γ Radiation Image Denoising Based on Speckle Splitting

Hao Deng[1,2], Hua Zhang[1,2*], Hao Zhao[2,3] and Hai Wang[1,2]

[1*]School of Information Engineering, Southwest University of Science and Technology, Qinglong Road, Mianyang, 621010, Sichuan, China.
[2]Special Environment Robot Technology Key Laboratory of Sichuan Province, Southwest University of Science and Technology, Qinglong Road, Mianyang, 621010, Sichuan, China.
[3]Department of Automation, University of Science and Technology of China, Huangshan Road, Hefei, 230026, Anhui, China.

*Corresponding author(s). E-mail(s): swustai@163.com;
Contributing authors: denghao@mails.swust.edu.cn;
zhaohao@swust.edu.cn; 596052009@qq.com;

Abstract

The images captured with CMOS sensor in γ radiation scene mainly affected by single-shot noise, induced noise and ionized air glow noise. In this paper, we propose a two-stage image denoising method based on speckle splitting to improve the clarity of the image originated from the γ radiation scene. Concretely, we first losslessly split the noisy image into multiple sub-images by dilated down-sampling, making the speckle noise in the original image decomposed into isolated point noise in the sub-images. Secondly, the median filtering is utilized to remove salient noise in sub-images. Lastly, aiming at the problem of incomplete denoising due to subtle differences between non-salient noises and background pixels. The gradient-guided NLM filtering in YUV color space is presented for second-stage denoising. Extensive experiments are carried out on the images captured from Co60 γ radiation scene. Compared with the original image, our method improves the PSNR by 8.17dB and SSIM by 0.32. Experimental

results demonstrate that the proposed method enjoys the state-of-the-art performance in improving the clarity of γ radiation image.

Keywords: γ radiation, speckle noise, image denoising, speckle splitting, NLM

1 Introduction

With the deepening exploration of human society in nuclear energy development, space exploration and artificial irradiation, the need for clear visualization of γ radiation scenes has become more and more urgent[1]. However, affected by the gamma photons, the image in gamma radiation environment becomes blurred due to the influence of speckle noise, which seriously interferes with the visual quality of the scene image, making denoising methods based on image processing has attracted a large amount of researchers[2, 3].

The noise in the γ radiation scene image mainly contain single-shot noise, induced noise and ionized air glow noise. As shown in Figure 1, the single-shot noise is shown as irregular white speckle in the elliptical region, the induced noise is shown as irregular black areas in the trapezoidal region, and the ionized air glow noise is shown as colored pixels in the rectangular region. Compton scattering between gamma photons and COMS sensors is the main cause of single-shot noise [4, 5]. The induced noise mainly caused by the Compton secondary electrons in conjunction with the image sensor Wide Dynamic Range (WDR). High-energy photons transfer a large amount energy to air molecules and make the air glowing, which is captured by COMS sensor and produce ionized air glow noise[6]. The aforementioned generation mechanisms of kinds of noise are the significant cues to remove them. There are three categories characteristics of noise.

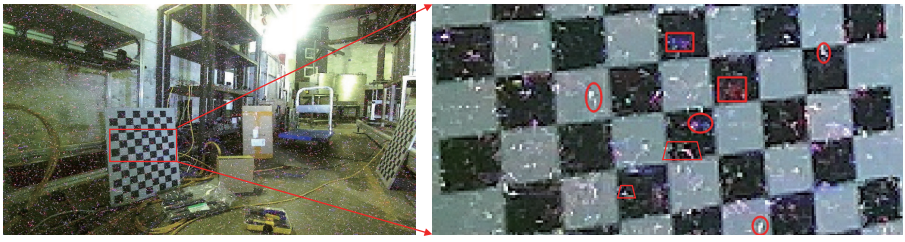

Fig. 1 Noise in the γ radiation image

The first is the geometric characteristic of noise. Due to the isotropic characteristic of radioactive source decay process, the incident angle and motion trajectory of high-energy photons acting on the CMOS sensor are independent of each other, which leads to the characteristic of noise with different shapes, random locations. Moreover, the density of speckle noise becomes denser with the increase of irradiation dose[1, 5, 7–10]. The geometric characteristics of

gamma radiation noise are applied to denoise the gamma radiation image from the perspective of local information association [11–13].

The second is the color characteristic of noise. To the best of our knowledge, the single-shot noise is mainly white patches and the induced noise is mostly black patches. The ionized air glow noise is mainly blue and reddish brown, and its appearance is closely related to the characteristic electromagnetic wave released by air molecules. In RGB color space, there is one channel of noise image which is much larger than the normal image at least. In [14–16], researchers utilize the median filter and its variants to improve the clarity of radiation image based on the color characteristics of gamma noise.

The last one is the temporal impulse characteristics of noise. Considering the transmission time of gamma photons in CMOS sensor is very short. Compared with the exposure time of CMOS, the influence of single photon does not have continuous characteristic for imaging result. That is, gamma radiation noise enjoys transient characteristics. In [17–19], motivated by the transient characteristics of gamma, Researchers exploit the sequence information to improve image quality.

In this paper, we mainly investigate how to improve the visual quality of radiation image from the perspective of noise generation mechanism. To this end, we propose a novel gamma radiation image denoising method based on speckle splitting. At first, speckle noise is decomposed into isolated point noise through dilated down-sampling. And then, a median filtering based on noise detection is proposed to repair the salient noisy pixels. Lastly, we apply gradient-guided non-local means (gradient-guided NLM) to reduce non-significant noise.

To summary, the main contributions of this paper can be concluded as follows:

- We present a novel two-stage gamma radiation image denoising method based on speckle splitting.
- We construct a non-salient noise reduction method by applying gradient-guided NLM filtering in YUV color space.
- Extensive experiments conducted on the true gamma radiation dataset show that the proposed method outperforms the state-of-the-art radiation image denoising approaches.

The rest of this paper is organized as follows: Section 2 introduces a brief review on recent work. Section 3 elaborates the implementation details of our proposed method. Extensive comparison experiments are carried out on the true gamma radiation dataset in Section 4. Last, a conclusion is drew in Section 5.

2 Related Works

In this section, we briefly review relevant works including temporal correlation denoising and spatial structure denoising.

2.1 Temporal Correlation Denoising

In the artificial irradiation facilities, nuclear power plant, etc., due to the imaging stationary, the scene images has the characteristics of background temporal correlation, while the γ radiation noise has transient characteristics. Many researchers have conducted a series of exploration of γ radiation noise removal based on the different characteristics between background pixels and noisy pixels. [19] performed noise detection and removal by subtraction and addition of adjacent images, which is effective for small isolated noise and unsatisfactory for dense speckle. [18] utilized temporal mean filtering to remove speckle noise in the nuclear reactor monitoring images. This way has the problem of detail blurring. [16] proposed a gradient difference denoising method based on the discrete characteristics of clean image and noisy image in time-domain and space-domain. This approach cannot remove subtle residuals. [17] constructed an average time-sequence method to remove gamma radiation noise by using the time sequence impulse characteristics of gamma noise. This method have a certain effect on single-shot noise and induced noise, but the performance on the ionized air glow noise is not desirable.

2.2 Spatial Structure Denoising

The premise of background fixation limits the application and development of temporal denoising methods, making spatial structure denoising methods that find the difference between noisy pixels and non-noisy pixels in an image attract more interest. [11] utilized the correlation degree of local details of image to detect and remove gamma noise, which has a good effect on the salient single-shot noise, but it cannot deal with air glow noise and induced noise. [13] applied NLM to denoise the nuclear medical images, which ignored the effects of the induced noise and airglow noise. [20] proposed a denoising method for nuclear medical noise image, called Bitonic filtering, which had a serious impact on the image details. [21] utilized the improved BM3D to remove the speckle noise in CT image. [22] applied the anisotropy filtering to denoise the DTI image. [12] treated the gamma noise as additive speckle noise and exploited the block difference minimization constraint to detect and remove noise. This type of methods had a good performance on small-scale speckle noise, but it cannot work well on the large-scale noise. [23] proposed a gamma noise detection and denoising scheme based on total variation, which is effective for single-shot noise and air glow noise, but the performance on the induced noise is not desirable. The median filter[15], Wiener filter[24] and wavelet transformer[14] are also used to remove the speckle noise in radiation image. However, these methods can only effectively deal with single-shot noise and induced noise, and cannot work well in the removal of ionized air glow noise.

In this paper, we apply dilated down-sampling strategy to divide speckle noise into isolated noise. Then, the detection based median filtering is used to remove the salient noise, including single-shot noise center and induced noise.

What's more, the gradient-guided NLM filtering in YUV color space is built to alleviate the problem of ionized air glow noise and the fine edge of single-shot noise.

3 Methodology

In this section, we elaborate the proposed gamma radiation image denoising method. As shown in Figure 2, there are three main parts in the denoising scheme, including speckle splitting, detection based median filtering, gradient-guided NLM filtering. Sec.3.1 depicts how to decompose the speckle noise to point noise through dilated down-sampling. Sec.3.2 describes the median filtering of salient noise in split sub-images. Last, the Laplace gradient-guided NLM filtering is designed for second-stage denoising, repairing the noisy pixels of speckle edge and non-significant ionized air glow noise.

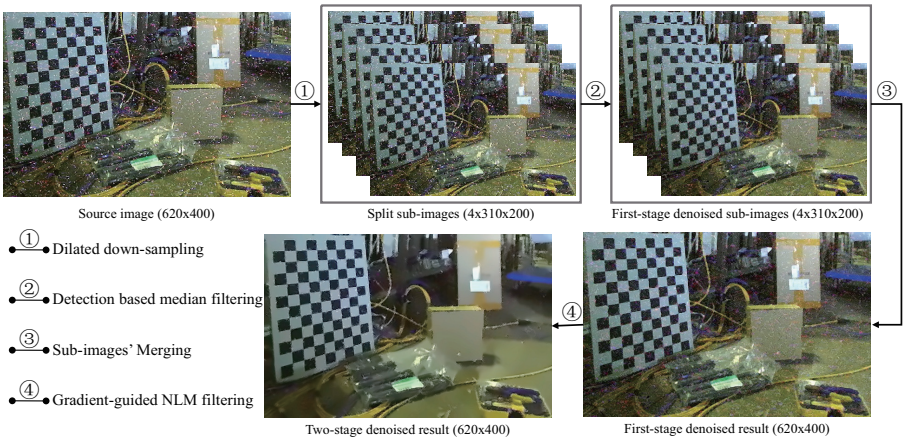

Fig. 2 An overview of the proposed γ radiation image denoising method

3.1 Speckle Noise Splitting

According to the geometric characteristics of γ noise, speckle noise has the characteristics of various geometric forms, random locations, and various size, resulting in it is difficult to accurately separate them from the background pixels with a suitable mathematical model. However, for whole scene image, the background pixels have a wide-range similarity property, that is, the pixel are similar in a larger range, while the γ noise has similarity only within the speckle and has strong differences with other pixels. So as shown in Figure 3, we use neighborhood dilation method for speckle splitting.

As shown in Figure 3(a), the γ radiation noise is distributed in patchy aggregates, and it is difficult to obtain the difference between the noise and the background pixels when performing spatial structure denoising, so the image

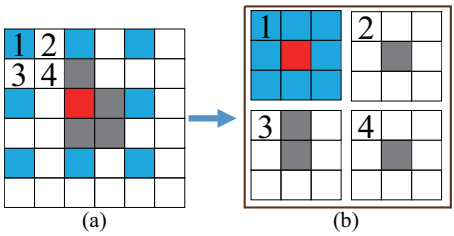

Fig. 3 The process of dilated down-sampling

is losslessly down-sampled into a set of sub-images as shown in Figure 3(b) by dilating the neighborhood of each pixel with radius r, and then sliding sampling in the original image. In the split sub-images, the speckle noise is easily isolated as point noise, and other pixels achieve a good preservation of image details.

For the input γ radiation image I, after the dilated down-sampling with radius r, the correspondence of pixels $S_i(x, y)$ between sub-images and original can be described as Eq.1.

$$S_i(x, y) = I\left((x \cdot r + i/r),\ (y \cdot r + i \backslash r)\right) \tag{1}$$

where i denotes the index of sub-images, and $\backslash$ is the modular operation.

3.2 Detection-based Median Filtering

Dilated down-sampling divide speckle noise into isolated point noise, and median filtering has excellent adaptability to this type of noise. However, conventional median filtering performs median substitution for each pixel, causing the background pixels to be blurred. In this paper, detection-based median filtering is used to remove point noise after splitting and preserve image details.

For the pixel $S_i(x, y)$ in sub-images, its 8-neighborhood pixels set $\mathbf{N}$ can be obtained by Eq.2.

$$S_i(x_2, y_2) \in \mathbf{N} \quad if\ (\|x_2 - x\| = 1\ or\ \|y_2 - y\| = 1) \tag{2}$$

Then the difference of pixel $S_i(x, y)$ and each pixel in $\mathbf{N}$ can be expressed as Eq.3.

$$C(x, y) = \sum_{c \in \{R,G,B\}} sgn\left(\|\mathbf{N}_k^c - S_i^c(x, y)\| - t_1\right) \tag{3}$$

where $C(x, y)$ denotes the difference between pixel $S_i(x, y)$ and neighborhood pixels, $k \in \{1, 2, \ldots, \|\mathbf{N}\|\}$, $sgn(x) = \begin{cases} 1 & if(x \geq 0) \\ 0 & otherwise \end{cases}$ is the sign function. Since the pixel in each neighborhood are not identical, the difference between the current pixel and other pixels is considered different only when the difference is greater than the threshold t_1.

According to the color characteristics of γ noise, noisy pixels are quite different from background pixels. However, due to the problem of incomplete

splitting during dilated down-sampling, some noisy pixels may still exist in the neighborhood, so the collective consistency principle shown in Eq.4 is adopted to judge the current pixel as noise when most of the neighborhood pixels are different from the current pixel.

$$R(x,y) = sgn\left(C(x,y) - \lambda \cdot \|\mathbf{N}\|\right) \tag{4}$$

where $\|\mathbf{N}\|$ denotes the number of neighborhood pixels. And λ is the scale factor, which determines the number of dissimilar pixels needed for the current pixel to be judged as noise.

After the current pixel is judged as a noisy pixel, in order to eliminate the interference of other noisy pixels on the median selection, the pixel points different from the current pixel are selected to the set of valid pixels, and the filtering method is shown in Eq.5.

$$\mathbf{N}_k \in \mathbf{N}^{\mathbf{V}} \quad if\left(\|\mathbf{N}_k^c - S_i^c(x,y)\| > t_1\right) \tag{5}$$

where $\mathbf{N}^{\mathbf{V}}$ is the set of the valid pixels, its median value is used to repair the noisy pixel in the sub-images. Then the denoised sub-images are inverse processed according to the down-sampling method to realize the first-stage denoising of γ radiation image.

3.3 Gradient-guided NLM Filtering

Although the detection based median filtering method effectively removes the salient noise, the problems of weak noise with little difference between speckle edges and background pixels, non-significant ionized air glow noise, and uneven local structure of the image after inverse down-sampling caused by the difference in the median selection of each sub-images are not well resolved. In this paper, after first-stage denoising, non-salient noise are detected and repaired using the Laplace gradient-guided NLM filtering in the YUV color space.

For the noisy block v_i in the input image I, NLM filtering[25] method globally finds multiple similar blocks v_j and then weights theses blocks to recovery v_i. Its mathematical description is shown as Eq.6.

$$NL(v_i) = \sum_{j \in I} \omega(i,j) \cdot v_j \tag{6}$$

where $\omega(i,j) = \frac{1}{Z(i)} e^{-\frac{\|v(N_i) - v(N_j)\|_{2,\sigma}^2}{h^2}}$ denotes the similarity weight coefficient between blocks v_i and v_j, and $Z(i) = \sum_j e^{-\frac{\|v(N_i) - v(N_j)\|_{2,\sigma}^2}{h^2}}$ is the normalization factor, σ is the standard deviation of Gaussian kernel, and h is the smoothing factor.

NLM method smooth fine noisy texture through non-local Gaussian filtering. However, the γ radiation image has a large number of background pixels in addition to the noisy pixels, and all pixels filtered by NLM will cause serious damage to the image details. Then the detection based denoising strategy is

still used in this section. According to the geometric characteristics of γ radiation noise, the distribution of speckle edge is messy, while the background pixels have certain structural characteristics, resulting in the Laplace gradient of noisy pixels in YUV color space more significant. Therefore, this paper detects and removes the non-salient noise in the YUV color space guided by Laplace gradient.

For the input γ radiation image I, the Laplace gradient $D^c \quad c \in \{Y, U, V\}$ in the YUV color space can be obtained by Eq.7.

$$D^c = \frac{\partial^2 I^c}{\partial x^2} + \frac{\partial^2 I^c}{\partial y^2} \tag{7}$$

then the Laplace gradient-guided NLM filtering method can be described by Eq.8.

$$NL(v_i) = \begin{cases} \sum\limits_{j \in I} \omega(i,j) \cdot v_j & if(D^c > t_2) \\ v_i & otherwise \end{cases} \tag{8}$$

where t_2 is the gradient threshold for the noisy pixels, and it is set to 80 by experiments on a large amount of γ radiation image.

4 Experiments

In this section, the proposed method is evaluated and compared with the state-of-the-art radiation image denoising approaches. The comparative experiments are conducted on the gamma radiation images which are collected by right camera of ZED 2 in the Co60 radiation chamber with a radiation dose of 110Gy/h, and all images are acquired when the camera was exposed to a Total Ionized Dose (TID) about 73.35Gy.

4.1 Experimental Configuration

To validate the effectiveness of the proposed method, we select state-of-the-art gamma-denoising methods Chen[23], Park[13], Treece[20] and Zhao[21] as the comparison methods. The parameters of each comparison method are configured with reference to the original configuration and carried out on the same platform (Laptop with Intel Core i5-7500@3.4GHz, 8G memory. IDE is Visual Studio 2015 @ OpenCV 4.2).

4.2 Metrics

Conventionally, we exploit two widely used metrics, Peak Signal to Noise Ratio (PSNR) and Structural Similarity (SSIM)[17], to measure the performance of our proposed method. As shown in Eq.9, PSNR represents the power ratio between signal and noise in the image. As depicted in Eq.10, SSIM synthesizes the brightness, contrast and structural similarity between the denoised image and non-noise image. The larger the values of above two metrics, the better the quality of the image.

$$\begin{cases} MSE = \frac{1}{M \cdot N} \sum_{i=0}^{M-1} \sum_{j=0}^{N-1} [I_d(i,j) - T(i,j)]^2 \\ PSNR = 10 \cdot \log_{10} \left(\frac{[max(I_d)]^2}{MSE} \right) = 20 \cdot \log_{10} \left(\frac{max(I_d)}{\sqrt{MSE}} \right) \end{cases} \tag{9}$$

$$\begin{cases} l(I_d, T) = \frac{2\mu_{Id}\mu_T + c_1}{\mu_{Id}^2 + \mu_T^2 + c_1} \ c(I_d, T) = \frac{2\sigma_{IdT} + c_2}{\sigma_{Id}^2 + \sigma_T^2 + c_2}, \ s(I_d, T) = \frac{\sigma_{IdT} + c_3}{\sigma_{Id}\sigma_T + c_3} \\ SSIM(I_d, T) = [l(I_d, T)]^\alpha \cdot [c(I_d, T)]^\beta \cdot [s(I_d, T)]^\gamma \end{cases} \tag{10}$$

4.3 Experimental Results

In order to clearly demonstrate the denoising effect of our method, several comparison experiments are conducted in real γ radiation images. The typical results are shown as Figure 4, and the quantitative evaluations are shown as Table 1.

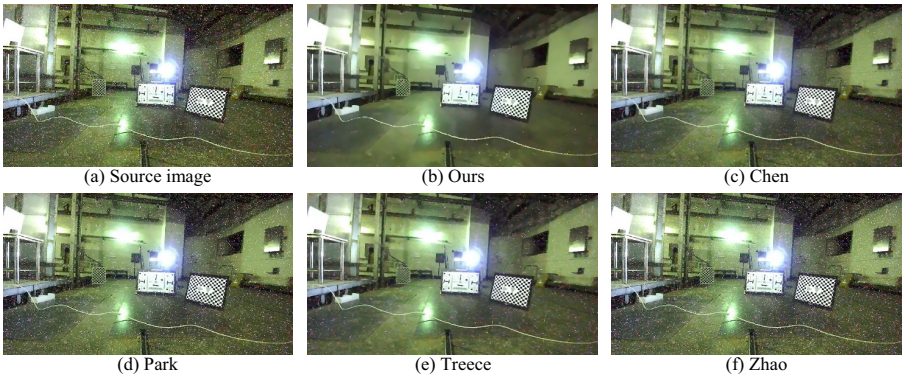

(a) Source image (b) Ours (c) Chen

(d) Park (e) Treece (f) Zhao

Fig. 4 Visual comparison of denoised image

Table 1 Quantitative comparisons of different denoising methods

Methods	Source	Ours	Chen	Park et al	Treece	Zhao et al
PSNR(dB)	19.80	**27.97**	26.21	20.27	25.70	19.87
SSIM	0.43	**0.75**	0.70	0.48	0.69	0.43

As shown in Figure 4 and Table 1, our proposed method achieves the best performance.

4.4 Ablation Studies

In order to verify the effectiveness of the denoising strategies, we conduct several ablation experiments on the radius r of dilated down-sampling, the

difference threshold t_1 and scale factor λ of the median filtering, the block scale c and smoothing factor h of the NLM filtering, as well as the first-stage denoising and second-stage denoising.

4.4.1 Effects of the dilation radius

Dilated down-sampling as the cornerstone of the denoising, the larger the dilation radius r, the more thorough the speckle splitting is, but at the same time, the greater the detail damage is. The denoising effects at different dilation radius is given in Figure 5, and the quantitative comparison is shown in Figure 6.

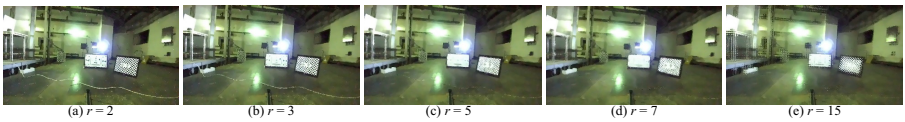

Fig. 5 Noise removal effects of dilation radius under different values

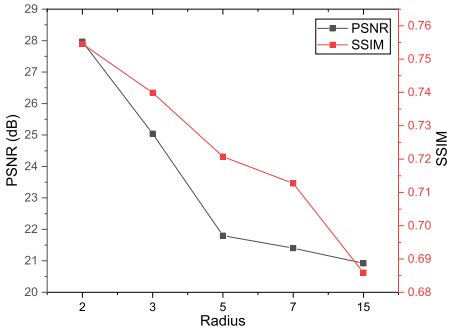

Fig. 6 Quantitative evaluation of dilation radius under different values

As shown in Figure 5 and Figure 6, the denoising method will obtain the best performance when r=2. In the case of images with more structured background pixels and fewer fine texture features, the dilation radius can be appropriately increased, but for applications with rich texture, a small dilation radius is better for retaining details.

4.4.2 Effects of the difference threshold and scale factor

The difference threshold t_1 is used as a baseline for the difference between noisy pixels and background pixels. A larger value requires a greater degree of difference between noise and background, and a smaller value can easily lead to the image edges being misclassified as noise pixels. And the scale factor λ is used to determine the outlier characteristic of center pixel and the neighboring pixels. The larger its value is, the more isolated the noise needs to be, and the

smaller its value is, the easier it is for the image edges to be misclassified as noise. The quantitative comparison at different difference threshold and scale factor is shown as Figure 7.

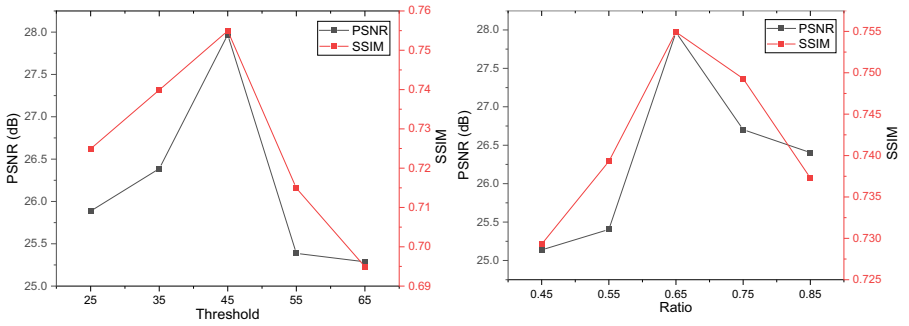

(a) Quantitative comparison of different t_1 (b) Quantitative comparison of different λ

Fig. 7 Quantitative comparison of difference threshold and scale factor under different values

As shown in Figure 7, proposed method achieved the best performance when t_1=45 and λ=0.65. The speckle center of γ radiation noise has strong impulse characteristics, so the difference threshold at 45 can well remove such salient noise and effectively retain the image details. Since the fixed dilation radius is difficult to adapt to the various size of the speckle noise, the scale factor is designed to detect the noise in the case of incomplete speckle splitting.

4.4.3 Effects of the block size and smoothing factor

NLM filtering finds and weights multiple similar blocks in original image for noise removal. It is difficult to find similar blocks if the block size is too large, and the noise cannot be completely removed if the block size b_s is too small. The smoothing factor h determines the weights of multiple similar blocks, the larger the value the better the denoising effect and the more likely to damage the image details, the smaller the value the better it is to retain the image details, but the effects of noise removal is insufficient. As shown in Figure 8, our method gets best results when b_s=7 and h=5.

4.4.4 Effects of the first-stage denoising and the second-stage denoising

The first-stage denoising includes speckle splitting and median filtering, while the second-stage denoising is NLM filtering. The dilation splitting divides the speckle noise into isolated point noise, and the salient noise are removed by median filtering, then the NLM filtering repairs non-significant noisy pixels. We compare the image denoising scheme without first-stage denoising, the image denoising scheme without second-stage denoising and ours, as shown in Figure

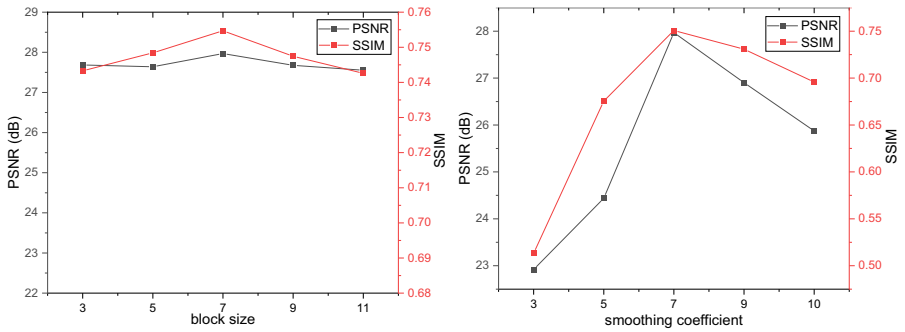

(a) Quantitative comparison of different b_s (b) Quantitative comparison of different h

Fig. 8 Quantitative comparison of block scale and smoothing factor under different values

9 and Table 2, the image denoising method combining first-stage denoising and second-stage denoising can achieve the best denoising performance.

(a) Source image (b) Splitting & Median (c) NLM (d) Splitting & Median & NLM

Fig. 9 Comparisons of visual effect with different denoising methods

Table 2 Quantitative Comparison of Ablation Studies

Splitting	Median	NLM	PSNR(dB)	SSIM
✓	✓		20.77	0.48
		✓	22.67	0.54
✓	✓	✓	**27.97**	**0.75**

5 Conclusion

In this paper, we propose an image denoising method based on speckle splitting to improve the clarity of the raw image originated from the γ radiation scene. We first decompose the speckle noise into isolated point noise by dilated downsampling. And then, the detection based median filtering is used to detect and remove salient noise. Meanwhile, we utilize gradient-based NLM filtering to repair non-significantly noisy pixels. Extensive experimental results demonstrate the effectiveness of our method. Specifically, compared with the original image, the PSNR of the proposed method is improved by 8.17dB and the SSIM is boosted by 0.32. In the future work, we will further investigate the temporal

characteristics of the noise and the background, and study the combination of temporal features and spatial structure for γ radiation image denoising.

Declarations

- Ethics approval and consent to participate. [Not applicable]
- Consent for publication. [Not applicable]
- Availability of data and materials. All data generated or analysed during this study are included in this submitted article.
- Competing interests. The authors declare that they have no known competing financial interests or personal relationships that could have appeared to influence the work reported in this paper.
- Funding. This work was supported by Sichuan Science and Technology Program (Grant No. 2021YFG0376/2021YFG0380).
- Authors' contributions. Hao Deng carried out the work related to γ radiation image acquisition, algorithm design and method implementation. Hao Zhao assisted in manuscript framework design and language revision. Prof. Hua Zhang provided full guidance on γ irradiation mechanism, data acquisition and mathematical methods. Hai Wang provided support in γ radiation image acquisition.
- Acknowledgements. Thanks to Special Environment Robot Technology Key Laboratory of Sichuan Province for providing the computing resources and analysis platform. I also thank my wife for her full support of my research.

References

[1] Belloir, J.-M., Virmontois, C., Estribeau, M., Goiffon, V., Magnan, P., Materne, A., Bardoux, A.: Radiation effects in pinned photodiode cmos image sensors: Variation of photodiode implant dose. IEEE Transactions on Nuclear Science **66**(7), 1671–1681 (2019). https://doi.org/10.1109/TNS.2019.2922659

[2] Sanada, Y., Kondo, A., Sugita, T., Nishizawa, Y., Yuuki, Y., Ikeda, K., Shoji, Y., Torii, T.: Radiation monitoring using an unmanned helicopter in the evacuation zone around the fukushima daiichi nuclear power plant. Exploration Geophysics **45**(1), 3–7 (2014). https://doi.org/10.1071/EG13004

[3] Ni, J., Chen, P., Li, S., Gao, X.: AP1000 radiation monitoring system design and engineering solution (2013)

[4] Yan, Z., Hu, Y., Huang, G., Dai, T., Zhang, Z., Wei, Q.: Detecting nuclear radiation with an uncovered cmos camera; a long-wavelength pass filter. In: 2019 IEEE Nuclear Science Symposium and Medical Imaging Conference (NSS/MIC), pp. 1–3 (2019). https://doi.org/10.1109/NSS/MIC42101.2019.9059807

[5] Wang, Z., Xue, Y., Chen, W., He, B., Yao, Z., Ma, W., Sheng, J.: Fixed pattern noise and temporal noise degradation induced by radiation effects in pinned photodiode cmos image sensors. IEEE Transactions on Nuclear Science **65**(6), 1264–1270 (2018). https://doi.org/10.1109/TNS.2018.2837015

[6] Arzaga-Barajas, E., Massillon-JL, G.: Thermoluminescent relative efficiency of tld-100 glow peaks after exposure to x-rays of 20 kv–300 kv, 137cs and 60co gamma. Radiation Measurements **146**, 106635 (2021). https://doi.org/10.1016/j.radmeas.2021.106635

[7] Virmontois, C., Belloir, J.-M., Beaumel, M., Vriet, A., Perrot, N., Sellier, C., Bezine, J., Gambart, D., Blain, D., Garcia-Sanchez, E., Mouallem, W., Bardoux, A.: Dose and single-event effects on a color cmos camera for space exploration. IEEE Transactions on Nuclear Science **66**(1), 104–110 (2019). https://doi.org/10.1109/TNS.2018.2885822

[8] Goiffon, V., Rolando, S., Corbière, F., Rizzolo, S., Chabane, A., Girard, S., Baer, J., Estribeau, M., Magnan, P., Paillet, P., Van Uffelen, M., Mont Casellas, L., Scott, R., Gaillardin, M., Marcandella, C., Marcelot, O., Allanche, T.: Radiation hardening of digital color cmos camera-on-a-chip building blocks for multi-mgy total ionizing dose environments. IEEE Transactions on Nuclear Science **64**(1), 45–53 (2017). https://doi.org/10.1109/TNS.2016.2636566

[9] Goiffon, V., Corbière, F., Rolando, S., Estribeau, M., Magnan, P., Avon, B., Baer, J., Gaillardin, M., Molina, R., Paillet, P., Girard, S., Chabane, A., Cervantes, P., Marcandella, C.: Multi-mgy radiation hard cmos image sensor: Design, characterization and x/gamma rays total ionizing dose tests. IEEE Transactions on Nuclear Science **62**(6), 2956–2964 (2015). https://doi.org/10.1109/TNS.2015.2490479

[10] Wang, Z., Huang, S., Liu, M., Xiao, Z., He, B., Yao, Z., Sheng, J.: Displacement damage effects on cmos aps image sensors induced by neutron irradiation from a nuclear reactor. AIP Advances **4**(7), 077108 (2014) https://arxiv.org/abs/https://doi.org/10.1063/1.4889878. https://doi.org/10.1063/1.4889878

[11] Cao, L., Liu, G., Deng, H., Deng, L., Zhou, B.: Method for eliminating γ radiation plaque noise in video surveillance image based on local correlation information. Atomic Energy Science and Technology, 1–10 (2022). https://doi.org/10.7538/yzk.2021.youxian.0355

[12] Lee, E.S., Loianno, G., Thakur, D., Kumar, V.: Experimental evaluation and characterization of radioactive source effects on robot visual localization and mapping. IEEE Robotics and Automation Letters **5**(2), 3259–3266 (2020). https://doi.org/10.1109/LRA.2020.2975723

[13] Park, C.R., Lee, Y.: Fast non-local means noise reduction algorithm with acceleration function for improvement of image quality in gamma camera system: A phantom study. Nuclear Engineering and Technology **51**(3), 719–722 (2019). https://doi.org/10.1016/j.net.2018.12.013

[14] Wang, H., Sang, R., Zhang, H., Xie, X.: A new image denoising method for monitoring in intense radioactive environment. Transducer and Microsystem Technologies **30**(11), 59–61 (2011). https://doi.org/10.13873/j.1000-97872011.11.031

[15] Ma, J., Song, G., Wang, Q., Zhang, J.: An impulse noise removing method in radiography. Acta Photonica Sinica **39**(11), 2107–2111 (2010)

[16] Li, H., Schillinger, B., Calzada, E., Yinong, L., Muehlbauer, M.: An adaptive algorithm for gamma spots removal in ccd-based neutron radiography and tomography. Nuclear Instruments and Methods in Physics Research Section A: Accelerators, Spectrometers, Detectors and Associated Equipment **564**(1), 405–413 (2006). https://doi.org/10.1016/j.nima.2006.04.063

[17] Deng, L., Liu, G., Deng, H., Cao, L.: γ-ray noise removal based on video time series correlation. Laser and Optoelectronics Progress, 1–17 (2022)

[18] Hosoya, N., Miyamoto, A., Naganuma, J.: Real-time image improvement system for visual testing of nuclear reactors. In: 2017 Fifteenth IAPR International Conference on Machine Vision Applications (MVA), pp. 1–4 (2017). https://doi.org/10.23919/MVA.2017.7986758

[19] Yang, B., Zhao, L., Deng, Q.: A novel anti-nuclear radiation image restoration algorithm based on inpainting technology. Journal of University of South China(Science and Technology) **30**(04), 56–61 (2016). https://doi.org/10.19431/j.cnki.1673-0062.2016.04.011

[20] Treece, G.: Morphology-based noise reduction: Structural variation and thresholding in the bitonic filter. IEEE Transactions on Image Processing **29**, 336–350 (2020). https://doi.org/10.1109/TIP.2019.2932572

[21] Zhao, T., Hoffman, J., McNitt-Gray, M., Ruan, D.: Ultra-low-dose ct image denoising using modified bm3d scheme tailored to data statistics. Medical Physics **46**(1), 190–198 (2019) https://arxiv.org/abs/https://aapm.onlinelibrary.wiley.com/doi/pdf/10.1002/mp.13252. https://doi.org/10.1002/mp.13252

[22] Li, P.: Dti image denoising algorithm based on anisotropic filtering. Master's thesis, Hebei University (2019)

[23] Chen, M.: Research on nuclear radiation contaminated image enhancement based on total variation and sparsity representation. PhD thesis, Southwest University of Science and Technology (2020)

[24] Lee, S., Lee, Y.: Performance evaluation of median-modified wiener filter algorithm in high-resolution complementary metal–oxide–semiconductor radio-magnetic x-ray imaging system: An experimental study. Nuclear Instruments and Methods in Physics Research Section A: Accelerators, Spectrometers, Detectors and Associated Equipment **1010**, 165509 (2021). https://doi.org/10.1016/j.nima.2021.165509

[25] Buades, A., Coll, B., Morel, J.-M.: Non-local means denoising. Image Processing On Line **1**, 208–212 (2011). https://doi.org/10.5201/ipol.2011.bcm_nlm